Available online at www.sciencedirect.com
ScienceDirect
Journal of Power Sources 178 (2008) 651–660
JOURNAL OF POWER SOURCES
www.elsevier.com/locate/jpowsour

New membranes based on ionic liquids for PEM fuel cells at elevated temperatures

H. Ye [a], J. Huang [a], J.J. Xu [a], N.K.A.C. Kodiweera [b], J.R.P. Jayakody [b,1], S.G. Greenbaum [b,*]

[a] *Department of Materials Science and Engineering, Rutgers University, Piscataway, NJ 08854, USA*
[b] *Department of Physics and Astronomy, Hunter College of the City University of New York, New York, NY 10021, USA*

Received 30 June 2007; received in revised form 28 July 2007; accepted 30 July 2007
Available online 9 August 2007

Abstract

Proton exchange membrane (PEM) fuel cells operating at elevated temperature, above 120 °C, will yield significant benefits but face big challenges for the development of suitable PEMs. The objectives of this research are to demonstrate the feasibility of the concept and realize [acid/ionic liquid/polymer] composite gel-type membranes as such PEMs. Novel membranes consisting of anhydrous proton solvent H_3PO_4, the protic ionic liquid $PMIH_2PO_4$, and polybenzimidazole (PBI) as a matrix have been prepared and characterized for PEM fuel cells intended for operation at elevated temperature (120–150 °C). Physical and electrochemical analyses have demonstrated promising characteristics of these H_3PO_4/$PMIH_2PO_4$/PBI membranes at elevated temperature. The proton transport mechanism in these new membranes has been investigated by Fourier transform infrared and nuclear magnetic resonance spectroscopic methods.

Keywords: Proton exchange membranes; Ionic liquids; Polybenzimidazole; NMR; FTIR

1. Introduction

Proton exchange membrane (PEM) fuel cells are considered one of the most promising technologies for stationary power generation, in addition to their leading role among all fuel cell technologies for transportation applications. The operation temperature limitation of current PEM fuel cell systems is mainly that of the membrane itself. The membranes presently available for PEM fuel cells are perfluorosulfonic acid (PFSA)-based membranes such as Nafion™, which exhibit good performance only at temperatures lower than 100 °C. The critical issue is that the proton conduction of perfluorosulfonic acid (PFSA)-based membranes is highly dependent on water present in the membrane [1]. To meet these targets, novel PEM must be developed which shows less humidity dependence and good thermal stability at elevated temperature, where water and thermal management as well as catalytic activity are much improved.

A common approach to improving water retention in membranes above 100 °C is to incorporate hydrophilic/hygroscopic inorganic additives, such as silica [2,3] and titanium dioxide [4] into PFSA membranes. Other additives as metal phosphates [5–7] (zirconium phosphates, boron phosphate), heteropolyacids [8–10] (phosphotungstic acid, silicotungstic acid, phosphomolybdic acid, etc.) not only increase the water uptake but also provide an extra proton transport pathway in the membranes, by modifying the pore/channel structure of the host polymer [11]. To improve thermal stability of the polymer backbone, aromatic sulfuric acid moieties have been studied as alternatives to PFSAs in a variety of polymers, including sulfonated polyphenylene [12], sulfonated polyimides [13], sulfonated poly benzimidazole [14], sulfonated poly (sulfones) [15] and sulfonated poly (ether ketones) [16], etc. However, all these sulfonated ionomer membranes are still vulnerable to the loss of conductivity upon loss of water. Water is essential for proton conductivity because it promotes dissociation of the proton from the hydrophilic sulfonic acid and provides highly mobile hydrated protons. Water also swells the membranes and allows

* Corresponding author.
E-mail address: steve.greenbaum@hunter.cuny.edu (S.G. Greenbaum).
[1] Permanent address: Department of Physics, University of Kelaniya, Kelaniya, Sri Lanka.

0378-7753/$ – see front matter © 2007 Elsevier B.V. All rights reserved.
doi:10.1016/j.jpowsour.2007.07.074

for bridging between ionic inclusions facilitating proton conductivity [17]. The operation of these sulfonated membranes is still limited to a temperature around 120 °C due to their water dependence.

For the operation of PEM fuel cell at $T \geq 150\,^{\circ}C$, a non-aqueous proton conductivity mechanism is required [17]. Phosphoric acid and imidazole are two candidates which show considerable proton conductivities in the pure state [18,19]. Phosphoric acid shows a very high degree of self-dissociation ($H_2PO_4^-$ and $H_4PO_4^+$), along with some condensation (H_3O^+ and $H_2P_2O_7^{2-}$). Pure phosphoric acid shows extremely high proton conductivity ($7.7 \times 10^{-2}\,S\,cm^{-1}$ at 42 °C) which may be ascribed to the correlated motion of the oppositely charged defects, $H_2PO_4^-$ and $H_4PO_4^+$; whereas, the mobility of phosphate species is relatively lower [19]. Savinell et al. reported on doping Nafion membrane with phosphoric acid to increase its conductivity at higher temperatures [20]. Complexes of phosphoric acid with different polymer (mostly basic polymers) have been studied as a new series of proton conducting membranes as reviewed by Schuster et al. [21]. Among them, H_3PO_4-doped polybenzimidazole (PBI) have been most widely studied, due to PBI's excellent thermal and chemical stability, and more interestingly the combination of the positive contribution to proton transport from its repeat unit, benzimidazole, one kind of heterocycle similar to imidazole [22–32]. The conductivity of liquid imidazole is around $10^{-3}\,S\,cm^{-1}$ at 90 °C, its melting point T_m. The proton mobility is a factor of ~4.5 higher than the molecular diffusion coefficient at T_m and the fast proton transfer mechanism involves a $Im\cdots ImH^+\cdots Im$ structure within a dynamical hydrogen bonding network [19]. Kreuer et al. reported proton conducting polymeric systems based on nitrogen-containing heterocycles, such as imidazole and pyrazole [33]. Benzimidazole has also been studied for anhydrous proton conducting material recently [34]. All these heterocycles are amphoteric molecules, i.e. proton donor/acceptor, and the mobility of protons in these complexes is similar to the situation in water containing systems but with better thermal and/or chemical stability [33]. However, the volatile property of these heterocycles still limits their application to relatively low temperature. Tethering imidazole directly to a polymer backbone gave unsatisfying results [21], but more recently, tethering the imidazole to a polysiloxane backbone *via* a flexible spacer shows promising results [35].

Despite the extensive efforts on high temperature membranes in recent years, so far none of the membranes developed meet all the requirements for operation of PEM fuel cells at 150 °C. In recent years, ionic liquids as a novel class of solvents have attracted extensive attention from different fields. Ionic liquids are room-temperature molten salts typically consisting of bulky, asymmetric organic cations and inorganic anions, and possess many especially attractive properties such as non-volatility, non-flammability, high thermal stability, high ionic conductivity and wide electrochemical stability window [36–39]. Recently, Watanabe and co-workers showed that some ionic liquids are electro-active for H_2 oxidation and O_2 reduction under non-humidifying conditions [40]. These results demonstrate that ionic liquids in principle can serve as the electrolyte for fuel cell reactions. However, no practical proton-conducting membranes based on ionic liquids for PEM fuel cells have been reported, although there have been some reports on utilizing ionic liquids to substitute water in Nafion^{TM} or directly as a liquid electrolyte for laboratory fuel cells [41,42].

This work aims to demonstrate the feasibility of the concept of [acid/ionic liquid/polymer] composite gel-type proton conducting membranes that can serve as practical membranes for operation of PEM fuel cells at 150 °C. PBI possesses excellent thermal and chemical stability as well as its base property which makes it easy to interact with acid components, so that PBI is more suitable to apply to high temperature membranes. However, significant phase separation occurs when mixing ionic liquid 1-ethyl-3-methylimidazolium triflate (EMITf) or 1-ethyl-3-methylimidazolium bis(trifluoromethanesulfonyl)imide (EMITFSI) with H_3PO_4 and PBI, resulting in inhomogeneous membranes as observed in the laboratory. Ionic liquid with dihydrogen phosphate anion ($H_2PO_4^-$) should be miscible well with H_3PO_4 in the view of their identical anions. Moreover, the introduced $H_2PO_4^-$ can function as proton acceptor and transfer medium. Thus new ionic liquid 1-propyl-3-methylimidazolium dihydrogen phosphate ($PMIH_2PO_4$) has been synthesized for our purpose with the additional consideration that imidazolium ionic liquids normally have good thermal stability and low viscosity. In this paper, the preparation and investigation of novel H_3PO_4/$PMIH_2PO_4$/PBI composite membranes is described to suggest their feasibility for PEM fuel cell operated at elevated temperature.

2. Experimental

Most chemicals purchased were from Aldrich. Hydrophilic ionic liquid, 1-methyl-3-propyl-methylimidazolium dihydrogen phosphate ($PMIH_2PO_4$), and polybenzimidazole (PBI) were synthesized in the lab and will be described in detail in the following sections as well the preparation of [acid/ionic liquid/polymer] composite gel-type proton conducting membranes.

2.1. Synthesis of hydrophilic ionic liquid $PMIH_2PO_4$

The synthesis of $PMIH_2PO_4$ ionic liquid follows a two-step procedure, quaternization and then anion exchange reaction. The synthesis process is shown in the Scheme 1. First, 1-methyl imidazole is reacted with 1-chloropropane to get *N*-methyl-*N*-propyl imidazole chloride and dried under vacuum at 70 °C for 24 h. Then room temperature ionic liquids were obtained by anion exchange reactions of *N*-methyl-*N*-propyl imidazole chloride with $NH_4H_2PO_4$. The ionic liquid product was purified, recrystallized and then dried under vacuum at 80 °C for 24 h and stored in a glove box filled with active Argon gas. Synthesized $PMIH_2PO_4$ is a highly viscous liquid at room temperature. Its flow ability increases fast after modest heating.

2.2. Synthesis of PBI

3,4-Diaminobenzidine, isophthalic acid, phosphorous pentoxide (P_2O_5), methanesulfonic acid (CH_3SO_3H) and triflu-

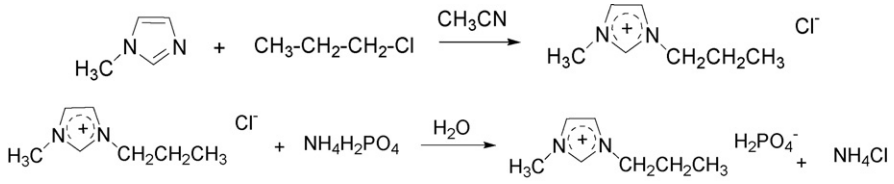

Scheme 1. Synthesis process of 1-methyl-3-propyl imidazolium dihydrogen phosphate.

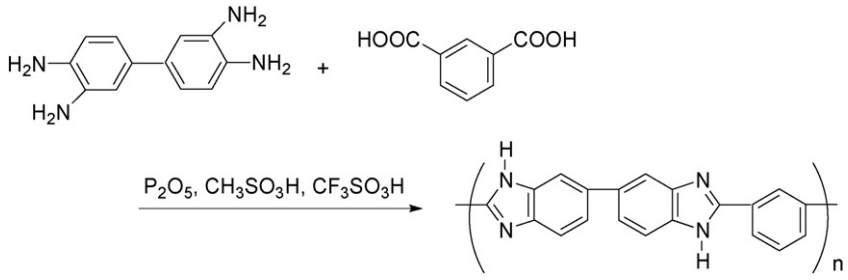

Scheme 2. Synthesis process of polybenzimidazole.

oromethanesulfonic acid (CF_3SO_3H) were purchased from Aldrich and used as received. The synthesis of PBI is based on reference [43] with some modification and the process is shown in Scheme 2. First, 1.21 g 3,3′-diaminobenzidine, 0.94 g isophthalic acid, 2 g P_2O_5, 7.5 ml CH_3SO_3H and 7.5 ml CF_3SO_3H were loaded into a 100 ml round bottom flask with stirring bar and reflux tube in the dry box. Second, the glassware setup was removed and the mixture stirred some more to make the reactants dissolve. Third, after heating the reaction mixture at 160 °C for 2 h a homogeneous solution was obtained and an increase of the solution viscosity was observed. Fourth, the viscous solution was added to deionized water under fast stirring; and powder or flake-shape products were precipitated out and collected. Fifth, the products were washed with water five times, then put into (150 ml) 10% $NH_3{\cdot}H_2O$, stirring overnight to remove the residual reactants, and then washed with water three more times. Finally, the yellow brown PBI powder was recrystallized from *N*,*N*-dimethylacetamide (DMAC) by chloroform ($CHCl_3$), then washed with water again and dried at 80 °C under vacuum for 24 h. FTIR analysis confirms that the synthesized product shows the characteristic peaks of PBI: 1626, 1533, 1444 cm^{-1}.

2.3. Preparation of [acid/ionic liquid/polymer] gel-type PEMs

H_3PO_4/$PMIH_2PO_4$/PBI polymer gel electrolyte membranes were prepared by a solution casting method. First, PBI was dissolved in DMSO with a concentration of 2 wt.%. Then proper amounts of H_3PO_4 or H_3PO_4/$PMIH_2PO_4$ with different mole ratios was added to PBI/DMSO solution and a viscous mixture solution resulted after stirring. The viscous mixture solution was cast over a Teflon tray and the DMSO was evaporated and a freestanding membrane resulted. The mole ratios of H_3PO_4/$PMIH_2PO_4$/PBI membranes chosen for study were 4/2/1, 3/3/1 and 2/4/1. For comparison, H_3PO_4/PBI and $PMIH_2PO_4$/PBI membranes have also been prepared using the same method and fixed at a mole ratio of H_3PO_4/PBI or $PMIH_2PO_4$/PBI equal to 4/1.

2.4. Membrane characterization

Thermogravimetric analysis (TGA) of the membranes was performed with a Perkin-Elmer TGA7. The measurement was carried out from room temperature to 300 °C under flowing N_2, with a heating rate of 10 °C min^{-1}. Differential scanning calorimetry (DSC) was performed with a Q1000 DSC System from TA Instruments, Inc. The measurement was carried out from −50 to 250 °C at a heating and cooling rate of 10 °C min^{-1}. A cooling–heating–recooling cycle was carried out first, and DSC data were collected during the second heating step. The ionic conductivity of the membranes was determined by the AC Impedance method, using a Solartron 1287 electrochemical interface combined with a 1260 impedance analyzer. The frequency range used for the impedance measurements was 1 MHz to 10 Hz and the amplitude was 5 mV. The conductivity cell Pt/membrane/Pt was assembled inside the glovebox, hermetically sealed and placed in an environment chamber (BMA, Inc.), which provided temperature control for the measurements. FTIR test was carried out using Bruker EQUINOX 55 Duroscope™ ATR.

For NMR measurements, samples were dried at 150 °C in a vacuum oven for 2 h and packed into 5 mm o.d. × 20 mm NMR tubes and flamed-sealed. NMR measurements were performed on a Chemagnetics CMX-300 spectrometer with ^1H Larmor frequencies of 301.02 MHz and a ^{31}P frequency of 121.85 MHz. Spectroscopic references were distilled water for ^1H and 85% H_3PO_4 for ^{31}P. Spectral information was obtained by Fourier transforming the resulting free-induction decay (FID) of single $\pi/2$ pulse sequence. Pulse widths were about 5 μs for ^{31}P and 12 μs for ^1H. Self-diffusion coefficients (D) were obtained by the NMR pulse gradient spin–echo technique (NMR-PGSE), using the Hahn spin–echo pulse sequence ($\pi/2 - \tau - \pi$) [44–46]. For a diffusing system in the presence

of a magnetic field the application of square-shaped magnetic gradients of magnitude g and duration δ results in attenuation of the echo amplitude A. This attenuation may be represented by $A(g) = \exp[-\gamma^2 g^2 D\delta^2(\Delta - (\delta/3))]$, where γ, D, δ, and Δ represent the nuclear gyromagnetic constant, self-diffusion coefficient, gradient pulse width, and gradient delay, respectively. Applied gradient strengths (g) ranged from 0.2 to 2.2 T/m, δ and Δ ranged from about 1 to 5 and 5 to 20 ms, respectively. The resulting echo profile versus gradient strengths is fitted to the above equation and D is extracted. Uncertainties in self-diffusion coefficient values are ~5%. Spin–lattice relaxation times (T_1) were evaluated from inversion recovery ($\pi - \tau - \pi/2$) [47] measurements. Variable temperature NMR measurements were made ranging from ambient to 180 °C, with equilibration times of 20–25 min following each temperature change.

3. Results and discussion

Fig. 1 shows the TGA of $PMIH_2PO_4$, H_3PO_4 and PBI. $PMIH_2PO_4$ is stable up to 250 °C, and H_3PO_4 and PBI are more stable than $PMIH_2PO_4$. Weight loss of the three components is less than 2 wt.% up to 150 °C. All components here meet the thermal stability requirements of elevated temperature operation.

H_3PO_4/$PMIH_2PO_4$/PBI membranes, with three designated compositions, i.e., the mole ratio of H_3PO_4/$PMIH_2PO_4$/PBI set at 4/2/1, 3/3/1 and 2/4/1, were prepared by solution casting method. The appearances of all prepared membranes are translucent brown, as shown in Fig. 2. H_3PO_4/$PMIH_2PO_4$/PBI membranes are flexible, elastic and freestanding. However, H_3PO_4/PBI (4/1) membrane is rather brittle and is difficult to handle; and $PMIH_2PO_4$/PBI (4/1) membrane is very elastic and sticky.

Fig. 3 shows the TGA of H_3PO_4/PBI, $PMIH_2PO_4$/PBI and H_3PO_4/$PMIH_2PO_4$/PBI membranes with different component molar ratio. All membranes demonstrate good thermal stability up to 200 °C and thus can be operated at elevated temperature. The weight loss of the membranes is less than 5.5 wt.% up to 200 °C except H_3PO_4/PBI (4/1) membrane. The somewhat higher loss than the previously quoted 2% probably includes products from the condensation of H_3PO_4 and/or $PMIH_2PO_4$ and some water uptake during the preparation of the sample for the TGA measurement.

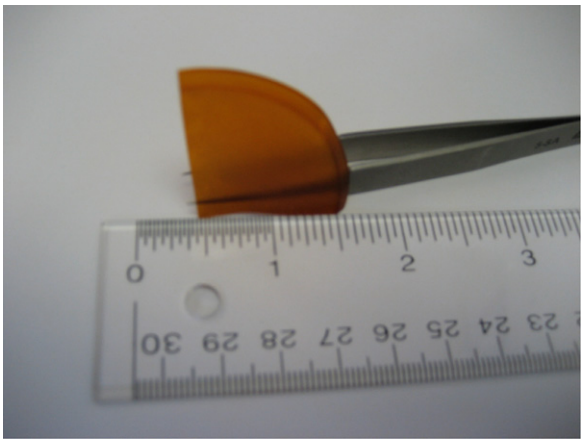

Fig. 2. Photograph of H_3PO_4/$PMIH_2PO_4$/PBI (2/4/1 here as an example) membrane.

Fig. 4 shows the DSC curves of H_3PO_4/PBI, $PMIH_2PO_4$/PBI and H_3PO_4/$PMIH_2PO_4$/PBI membranes with different component molar ratio. There is no significant phase transformation between room temperature to 200 °C. Apparently, the freezing/melting of H_3PO_4 and $PMIH_2PO_4$ has been suppressed, indicating strong interactions between the different components. There is a small curvature change for different membranes occurring at 36 °C for H_3PO_4/PBI, −25 °C for $PMIH_2PO_4$/PBI, and 32 °C, 28 °C, −5 °C for H_3PO_4/$PMIH_2PO_4$/PBI membrane with the mole ratio of 4/2/1, 3/3/1, and 2/4/1, respectively. This curvature change temperature point is most likely the glass transition of the membrane and the trend is consistent with the brittleness of the membrane. For example, the membrane with high content of $PMIH_2PO_4$ shows a lower curvature change temperature point and is more flexible. This indicates $PMIH_2PO_4$ plasticizing the PBI film. The fact that the membranes remain in a single

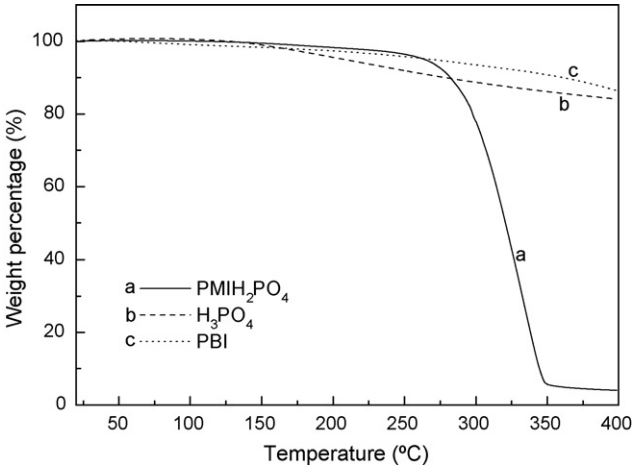

Fig. 1. TGA of H_3PO_4 and lab-synthesized $PMIH_2PO_4$ and PBI.

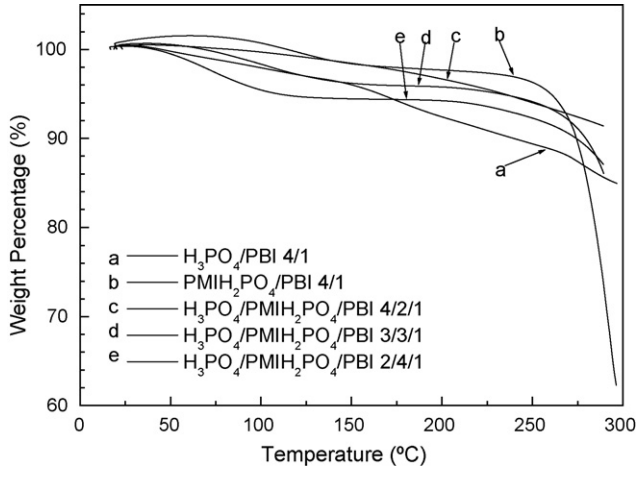

Fig. 3. TGA of H_3PO_4/PBI, $PMIH_2PO_4$/PBI and H_3PO_4/$PMIH_2PO_4$/PBI membranes.

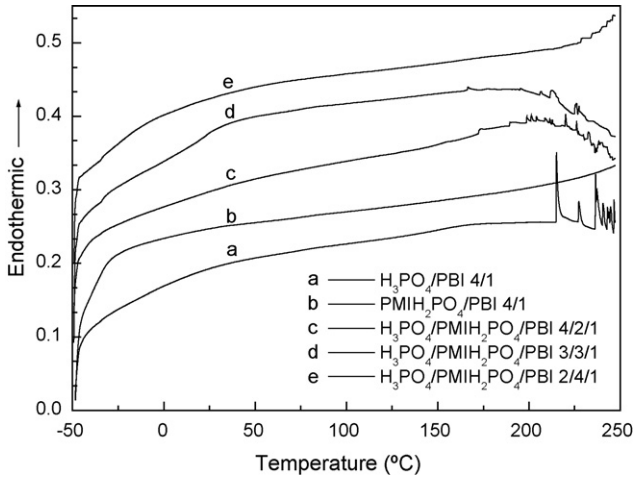

Fig. 4. DSC curves of H_3PO_4/PBI, $PMIH_2PO_4$/PBI and H_3PO_4/$PMIH_2PO_4$/PBI membranes (reheat step, 10 °C min^{-1} under N_2 atmosphere).

phase in the wide range of temperature is very important for fuel cell operation.

Fig. 5 displays the Arrhenius plot of ionic conductivity of H_3PO_4/PBI, $PMIH_2PO_4$/PBI and H_3PO_4/$PMIH_2PO_4$/PBI membranes with different component molar ratio. H_3PO_4/PBI and H_3PO_4/$PMIH_2PO_4$/PBI membranes exhibit similar temperature dependent conductivity and following VTF behavior [48–50], which indicates these membranes have similar ionic conduction mechanisms. However, the conductivity of $PMIH_2PO_4$/PBI membrane has weaker temperature dependence at temperature higher than 80 °C. In this particular sample there is probably a negligible proton contribution to the total ionic conductivity. Incorporating ionic liquid into H_3PO_4/PBI complex significantly increases the ionic conductivity of the membranes; a higher content of $PMIH_2PO_4$ yields a higher ionic conductivity for the membrane. Under completely anhydrous conditions, these H_3PO_4/$PMIH_2PO_4$/PBI membranes with 4/2/1, 3/3/1, and 2/4/1 compositions exhibit conductivities 0.84, 1.40 and 2.04 mS cm^{-1} at 150 °C, respectively.

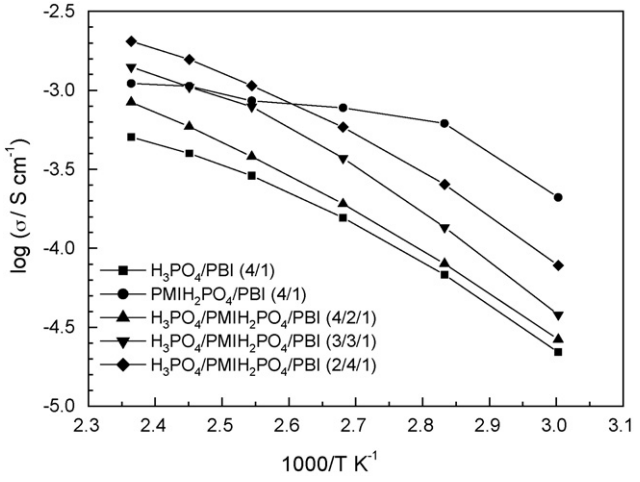

Fig. 5. Temperature dependent ionic conductivity of H_3PO_4/PBI, $PMIH_2PO_4$/PBI and H_3PO_4/$PMIH_2PO_4$/PBI membranes under anhydrous condition.

Table 1
Humidity effects on the ionic conductivity of H_3PO_4/$PMIH_2PO_4$/PBI membrane at 80 °C

Relative humidity (%)	H_3PO_4/$PMIH_2PO_4$/PBI (2/4/1) (mS cm^{-1})
0	0.254
10	0.90
20	1.31

Water vapor also has a dramatic effect on the ionic conductivity of the H_3PO_4/$PMIH_2PO_4$/PBI membranes. The film was stored under different humidity condition (0%, 10% and 20%) for 6 h at 80 °C at which temperature conductivity measurements were then made. Table 1 lists the humidity dependence of ionic conductivity of the H_3PO_4/$PMIH_2PO_4$/PBI membranes (2/4/1 here as example). It is found that the ionic conductivity of the membrane increase by more than a factor of two under relative humidity of 10% and more than four times under relative humidity of 20%. Considering water is the unavoidable by-product of PEM fuel cell reaction, the ionic conductivity for the H_3PO_4/$PMIH_2PO_4$/PBI membrane in an operating fuel cell could be substantially higher than in the absence of water.

The molecular vibration properties of H_3PO_4/PBI, $PMIH_2PO_4$/PBI and H_3PO_4/$PMIH_2PO_4$/PBI membranes have been studied by FTIR in the spectrum range 4000–400cm^{-1} as shown in Fig. 6. In the regions 3800–2000 cm^{-1} the NH and CH stretching modes (υ(N–H) and υ(C–H)) are expected to occur. As shown in Fig. 6(a), the broad peak centered at 3370 cm^{-1} was attributed to the stretching vibration of the NH groups involved in hydrogen bonding [28,51]. The sharp peaks around 3150, 3060, 2964, and 2877 cm^{-1} were attributed to stretching vibration of C–H on PMI cations and PBI [51–53]. A very broad absorption band appears around 2700 and 2300 cm^{-1} is related to the protonation of the nitrogen of the PBI and assigned to the υ(N^+–H) stretching mode [28,29]. As seen from Fig. 6(a), in the case of H_3PO_4/PBI complex, there are only very broad peaks around 2700 and 2300 cm^{-1} indicating a strong acid–base interaction between H_3PO_4 and PBI, with the nitrogen of the imide group acting as a strong proton acceptor. In the case of $PMIH_2PO_4$/PBI complex, the protonation peaks disappear but a broad peak around 3370 cm^{-1} occurs indicating there is weak interaction between $PMIH_2PO_4$ and PBI with a lesser degree of protonation. In the case of H_3PO_4/$PMIH_2PO_4$/PBI systems, the intensity of the 3370 cm^{-1} peak increases and the protonation peaks shift to higher wave numbers with increasing $PMIH_2PO_4$ due to the decreased acid strength of $PMIH_2PO_4$. As a result, adding $PMIH_2PO_4$ can adjust the acid–base interaction strength between H_3PO_4 and PBI and modify the hydrogen bonding strength, especially N···H–O bonding.

The intense absorption bands in the 1200–400 cm^{-1} spectral region are characteristic of the anions. C–H out-of-plane vibration, heterocyclic-ring vibration and benzene-ring vibration are also reflected in this region. Carefully comparing the IR spectra of ($C_2H_9N_2$) H_2PO_4, $PMIPF_6$ and PBI, it is concluded that 964 cm^{-1} peak is attributed to $P(OH)_2$ asymmetric stretching and the 460 cm^{-1} peak is assigned to PO_2 torsion [51,52,54]. Fig. 6(b) shows that there are different anion vibra-

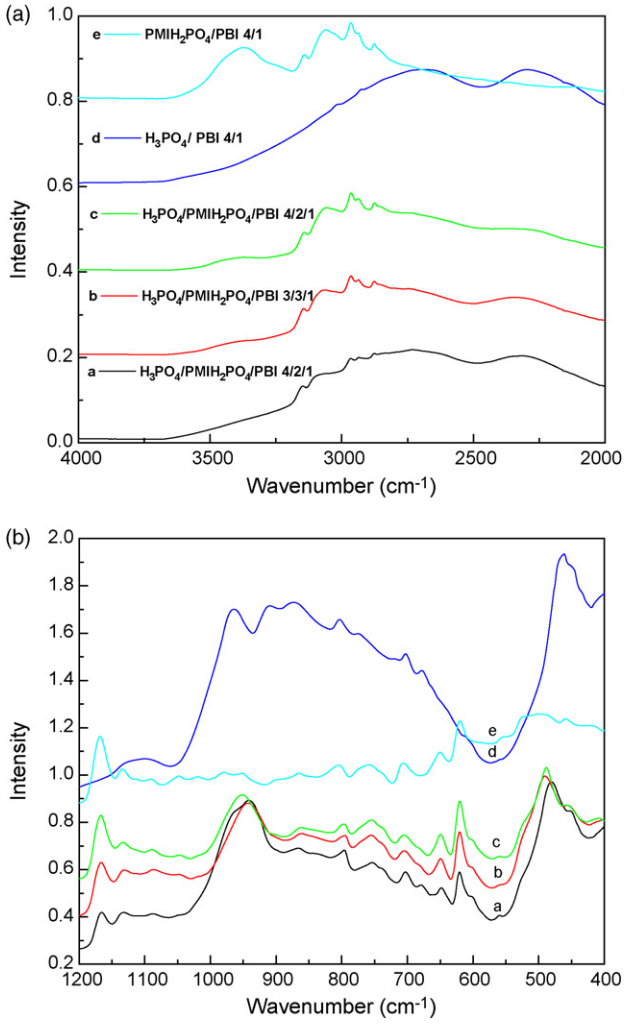

Fig. 6. FTIR absorption spectra of H_3PO_4/PBI, $PMIH_2PO_4$/PBI and H_3PO_4/$PMIH_2PO_4$/PBI membranes (3800–2000 and 1200–400 cm^{-1} region).

tional characteristic among H_3PO_4/PBI, $PMIH_2PO_4$/PBI and H_3PO_4/$PMIH_2PO_4$/PBI membranes, particularly with regard to the peak position and intensity of $P(OH)_2$ asymmetric stretching and PO_2 torsion modes. These results indicate that adding $PMIH_2PO_4$ also modifies the anion structural characteristics, such as bond strength and PO_4^- flexibility, which in turn leads to a change of the hydrogen bonding structure between H_3PO_4 and $PMIH_2PO_4$.

Fig. 7 displays ^1H spectra for four different ratios of H_3PO_4/$PMIH_2PO_4$/PBI. The spectrum 0/1/0 is for the pure ionic liquid ($PMIH_2PO_4$) shown for reference purposes. A detailed spectral assignment will not be given here, as the main purpose is to identify the dynamics of the various mobile species. Briefly, the largest feature (including the "shoulder") of the ionic liquid spectrum centered around −4.8 kHz from the reference frequency is assigned to the *N*-propyl and *N*-methyl protons, the peak roughly in the middle (around −3 kHz from the reference) is assigned to imidazole ring protons and the feature around 0 kHz is attributed to POH protons of the $H_2PO_4^-$ anion. The assignments of the membrane NMR spectra can thus be made, assuming that the rigid PBI protons contribute no more than a

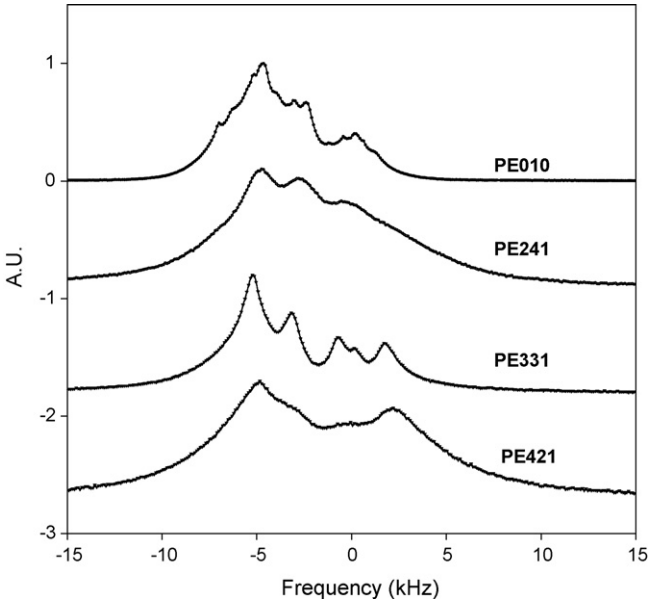

Fig. 7. ^1H Spectra of reference ionic liquid and membranes at 295 K, where the numbers *xyz* are the mole ratios of H_3PO_4, ionic liquid, and PBI, respectively.

broad baseline to the spectrum, on the basis of what happens when H_3PO_4 is added. Clearly, the addition of H_3PO_4 gives a spectral contribution +2 kHz from the reference. In this manner, monitoring the relaxation recoveries and diffusive decays of the *N*-alkyl protons and the H_3PO_4 will permit dynamical analysis of the IL cation and acid protons, the latter being of more direct relevance to membrane performance in a fuel cell. This argument does not yet take into account the effect of exchange between the protons of the IL anion and the H_3PO_4, which will be addressed later.

Arrhenius plots of ^1H T_1 of PMI and H_3PO_4 for H_3PO_4/$PMIH_2PO_4$/PBI membrane samples are displayed in Figs. 8 and 9, respectively. All mobile species exhibit T_1 minima between 125 and 145 °C. A T_1 minimum occurs when the motional correlation time is comparable to the reciprocal

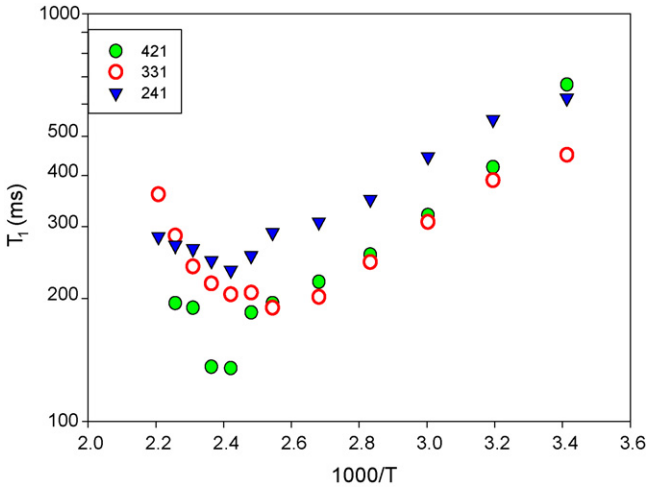

Fig. 8. NMR ^1H T_1 relaxation results for IL site of H_3PO_4/$PMIH_2PO_4$/PBI membranes. Again, the numbers *xyz* are the mole ratios of H_3PO_4, ionic liquid, and PBI, respectively.

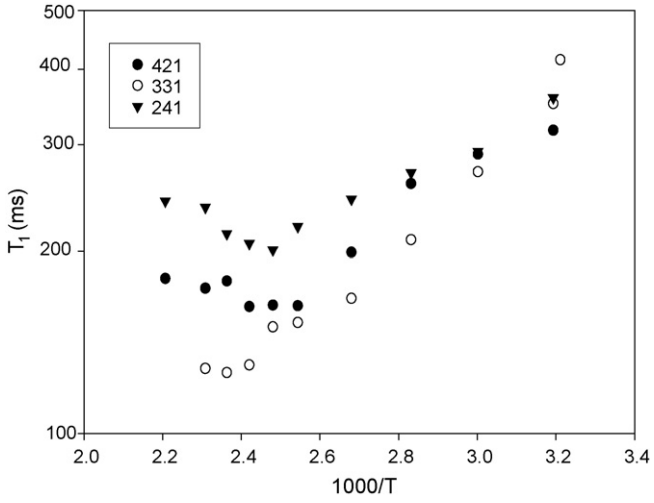

Fig. 9. NMR ^{1}H T_1 relaxation results for phosphate-associated protons in $H_3PO_4/PMIH_2PO_4$/PBI membranes.

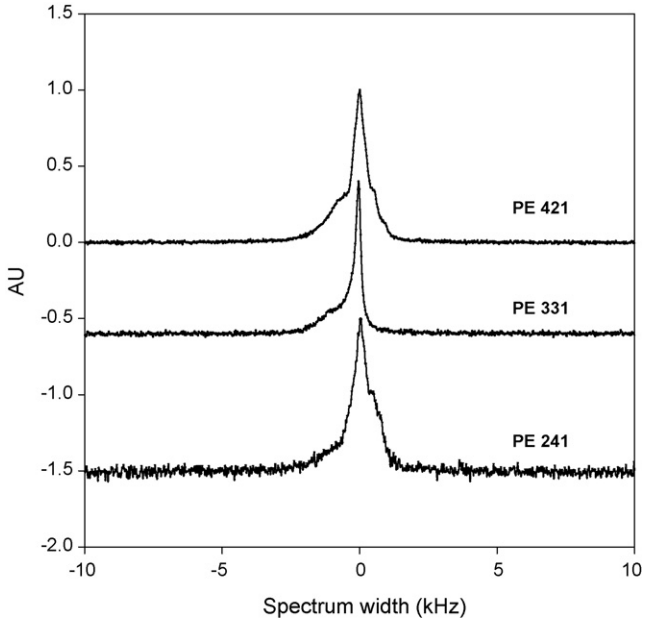

Fig. 10. ^{31}P NMR spectra of $H_3PO_4/PMIH_2PO_4$/PBI membranes.

of the Larmor angular frequency (in the present case, around 10^{-9} s) [47]. Thus it can be concluded that on the whole, all mobile species are dynamically correlated, which in turn suggests that the H_3PO_4 is well mixed with the ionic liquid phase on the nanoscale. In addition to short range translational motion, methyl group rotation can also provide an efficient relaxation mechanism. However there are subtle differences between the relaxation behaviors of the different proton sites in a given compound and between proton sites among the various membranes. In particular, local motion of the *N*-alkyl protons in the 3/3/1 membrane is enhanced as evidenced by its lower temperature T_1 minimum, which is consistent with smaller linewidths of individual components of this compound (Fig. 7). On the other hand, the POH protons in the 3/3/1 membrane exhibit a higher temperature T_1 minimum. The short range motions responsible for relaxation likely includes H^+ hopping between POH sites.

^{31}P spectra at 100 °C of $H_3PO_4/PMIH_2PO_4$/PBI membranes are shown in Fig. 10. All three spectra exhibits two main peaks with a relatively narrow component at the reference frequency indicating some amount of H_3PO_4 and the broad peak is attributed to the short range intermixing of H_3PO_4 with PBI and the IL. T_2 values of three different membranes were measured and they are short, about 1–2 ms over the temperature range of 20–180 °C. The broad line width and short T_2, even at high temperature, is attributed to the greater restriction of both translational and rotational phosphate group motion by the strong interaction with the host structure.

Arrhenius plots of ^{31}P T_1 for $H_3PO_4/PMIH_2PO_4$/PBI samples are displayed in Fig. 11 and it is clear that the spin–lattice relaxation is quite similar among the materials, an indication of the close similarity of the local environment of the phosphate ions in all samples. A T_1 minimum is observed in the 2/4/1 membrane and is believed to occur above the temperature range of this investigation for the other two compounds. Low T_1 values at higher temperature also contribute to the ^{31}P linewidth *via* lifetime broadening.

Proton diffusion results for $H_3PO_4/PMIH_2PO_4$/PBI samples, extending to 180 °C are displayed in Fig. 12. The values are presented for two main peaks, corresponding to the *N*-alkyl protons and the POH protons. As expected, the diffusion coefficients increase with increasing temperature. The diffusion values of POH are higher that those of IL cation for all three samples, with the largest difference occurring for PE_{241}. Previous studies of pure H_3PO_4 and H_3PO_4 in water have shown that the phosphate ions diffuse through a vehicular mechanism that depends on the solution viscosity, whereas acid protons diffuse *via* a hopping mechanism that is uncorrelated with viscosity [55]. In the present case, it is surmised that the IL cationic motion is vehicular while the acid protons also have a hopping pathway available. This may include rapid exchange between protons in the H_3PO_4 and the IL anion. The lack of clear resolution between the POH from the ionic liquid and the POH from the phosphoric

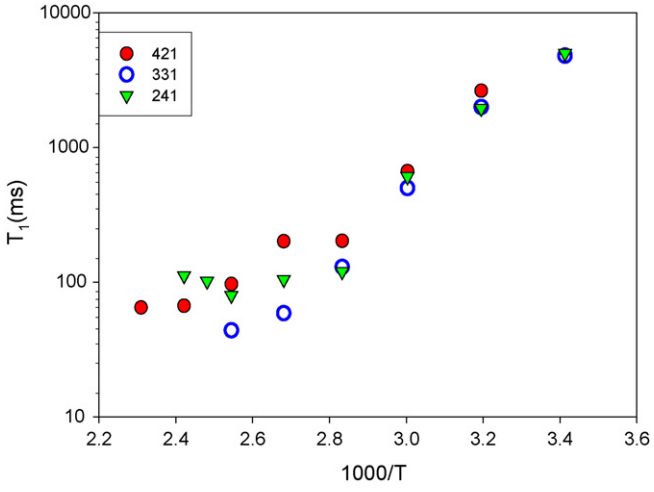

Fig. 11. NMR ^{31}P T_1 relaxation results for the acid site of $H_3PO_4/PMIH_2PO_4$/PBI membranes.

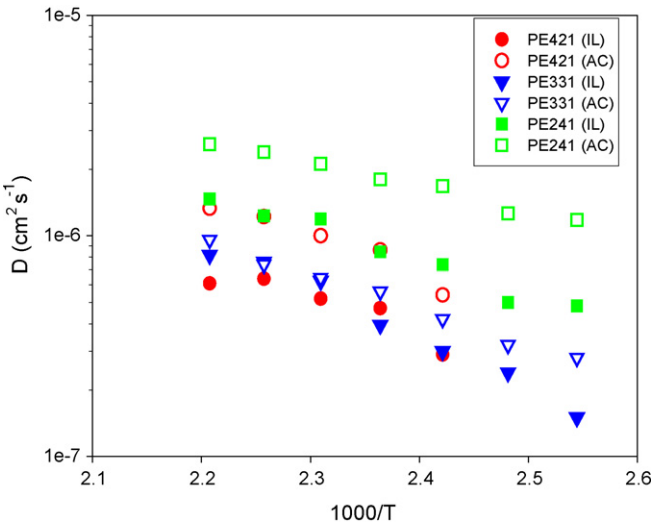

Fig. 12. Temperature dependence of the proton diffusion in H_3PO_4/$PMIH_2PO_4$/PBI membranes.

acid (Fig. 7) is consistent with proton exchange between these species, not unlike what has been observed in other phosphoric acid/PBI membranes where more than one phosphate species is present [56].

Although the diffusion coefficients have the highest value for the membrane with the highest ionic liquid concentration (PE_{241}), the next highest values occur for the membrane with the lowest IL concentration (PE_{421}). It is interesting that the intermediate IL concentration membrane (PE_{331}) gives the smallest difference between diffusion values of IL cation and acid protons, suggesting strong interactions among all components.

It was not possible to measure the ^{31}P diffusion coefficient of the membranes due to the short T_2 (1–1.5 ms) values, over entire temperature range. Given the highest value of $T_2 \approx 2.0$ ms observed for the membrane, which occurred at high temperature, and experimental limitations on gradient strengths, it is possible to estimate an upper limit of D that is consistent with the lack of observable echo decay, and that value is about 10^{-8} cm^2 s^{-1}. Thus there is negligible phosphate diffusion in these materials; i.e. about two orders of magnitude lower than the proton diffusion coefficients.

The ionic liquid will disperse homogeneously into the H_3PO_4/PBI complex due to its same anion as H_3PO_4. Combined with the good thermal and chemical stability of PMI^+ cation, it is reasonable to conclude that incorporating $PMIH_2PO_4$ will not compromise the advantages of H_3PO_4-doped PBI membranes such as good proton conductivity, zero electro-osmotic water drag number, low gas permeability, and excellent oxidative and thermal stability [22–32]. Moreover, it is expected that there would be a three-dimensional hydrogen bonding network within the H_3PO_4/$PMIH_2PO_4$/PBI membranes and proton conduction would occur mainly through the hydrogen bonding network by a hopping mechanism.

It is reported that $H_2PO_4^-$ anion has a strong tendency to form an infinite network (like chain, ribbons, layers, and three-dimensional network) *via* strong hydrogen bonds (O–H···O) in numerous structures of monophosphates with organic cations (most are heterocycles) [54]. Strong hydrogen bonding between H_3PO_4 and N and/or NH group of PBI (O–H···N and N–H···O) has also been demonstrated by infrared spectroscopy in the preceding section and in the literature [28,29,57]. It is then sensible to conclude that the whole H_3PO_4/$PMIH_2PO_4$/PBI complex is a three-dimensional H-bonded network which augments the structural integrity of the membrane and enhances its acid/ionic liquid stability. Moreover, the large number of defect protons, $H_2PO_4^-$ ions from the ionic liquid, themselves will increase the proton conductivity in the membranes due to their proton accepting nature, functioning as a proton exchange site [18]. Defect protons show fast structural diffusion comprising proton transfer with undissociated molecules (e.g. H_3PO_4) and structural reorganization of the PO_4-tetrahedra as discussed by Dippel et al. [58]. Therefore, this three-dimensional H-bonded network provides a medium in which the Grotthuss hopping mechanism plays an important role [57,59]. The proton transport in this H-bonding network can be schematized as in Fig. 13. Furthermore, the ionic liquid plasticizes the PBI chain and thus the membrane, facilitating the segmental motion of PBI and the reorganization of the PO_4-tetrahedra thus enhancing proton transfer of within the membranes as supported by the previously discussed FTIR analysis. Another role $PMIH_2PO_4$ may play is to adjust the strength of hydrogen bonding in the systems which may be optimized for proton transport. Kreuer et al. pointed out that dynamical bond-length variations are the key to long-range proton transport [18,19]. Strong hydrogen bonding is a prerequisite for proton transfer reaction; however, weak hydrogen bonding facilitates bond breaking and reforming so as to realize long-range proton transport [19]. Due to strong acid–base interaction between H_3PO_4 and PBI, PBI can be partially protonated by H_3PO_4 [28,57], with limited associated proton transport. But relatively weaker hydrogen bonding between $PMIH_2PO_4$ and PBI may balance this effect. Our FTIR analysis supports this hypothesis as does the proton exchange effects implied by the NMR results. The improvement of conductivity by increasing

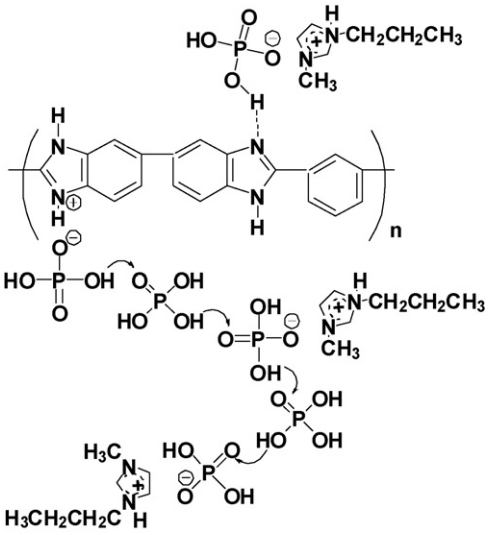

Fig. 13. Scheme of the proton conduction mechanism in the H_3PO_4/$PMIH_2PO_4$/PBI membranes under anhydrous condition.

the relative humidity can be ascribed to the bridging effect of water molecules in the proton conduction [59]. Also the membranes, all components of which are hygroscopic, absorb water which is an unavoidable by-product of fuel cell operation, and this further enhances proton conductivity.

In the H_3PO_4/$PMIH_2PO_4$/PBI membrane, though there are several mobile ions including PMI^+ cation and $H_2PO_4^-$ anion, only proton transport is relevant for fuel cell power production, other two will only induce the polarization of the fuel cell. The ^1H NMR diffusion results (Fig. 12) suggest that proton transport is the main contribution to the total ionic conductivity of the membranes. Tests in fuel cells and other analysis are yet to be carried out to evaluate these materials further. Of course, whether the thermal, mechanical and chemical stability of H_3PO_4/$PMIH_2PO_4$/PBI membranes is sufficient to maintain a satisfactory performance after long-term operation still needs to be established. It is noteworthy that the PBI/H_3PO_4 ratio in these membranes is considerably higher than reported for earlier systems (without ionic liquids). [27–29,59]. One limitation of those materials is leaching of the acid during long-term operation. Therefore, the retention of H_3PO_4 acid and $PMIH_2PO_4$ ionic liquid in fuel cells made with the current membranes also has to be established under long-term operating conditions. This is particularly relevant if even higher ionic conductivity is sought by means of increasing the acid and ionic liquid concentration.

4. Conclusions

[Acid/ionic liquid/polymer] polymer gel electrolyte membranes have been synthesized and characterized as prospective proton exchange membranes for PEM fuel cells operating at elevated temperature. Novel H_3PO_4/$PMIH_2PO_4$/PBI composite gel-type proton conducting membranes have been prepared using lab synthesized thermal engineering polymer polybenzimidazole (PBI) and ionic liquid, $PMIH_2PO_4$, with the proton accepting anion $H_2PO_4^-$. The investigated H_3PO_4/$PMIH_2PO_4$/PBI membranes are homogeneous, flexible, freestanding and with good thermal stability and wide temperature range of single phase behavior. The membranes have acceptable ionic conductivity of up to 2.0×10^{-3} S cm^{-1} at 150 °C and under anhydrous condition. The conductivity rises even higher when the membranes absorb some water vapor. H_3PO_4/$PMIH_2PO_4$/PBI membranes combine the advantage of H_3PO_4-doped PBI and special features of ionic liquid $PMIH_2PO_4$. A three-dimensional hydrogen bonding network structure inside of the H_3PO_4/$PMIH_2PO_4$/PBI membranes is proposed and proton conduction occurs mainly through the hydrogen bonding network by a hopping mechanism. The ionic liquid $PMIH_2PO_4$ is surmised to function as proton transfer bridges, a plasticizer for PBI, a balancer of the strengths of hydrogen bonding in the system, and an absorber and retainer of water. FTIR and NMR analyses support these hypotheses. It is suggested that further characterizing of these new membranes by other analytical techniques and under real fuel cell operating conditions is warranted.

Acknowledgments

The portion of this work carried out at Rutgers University was supported by the Energy Innovations Small Grant Program of the California Energy Commission. The portion of this work carried out at Hunter College was supported in part by grants from the U.S. Air Force Office of Scientific Research and the U.S. Department of Energy.

References

[1] M. Cappadonia, S.M.S. Niaki, U. Stimming, Solid State Ionics 77 (1995) 65.
[2] P.L. Antonucci, A.S. Arico, P. Creti, E. Ramunni, V. Antonucci, Solid State Ionics 125 (1999) 431.
[3] S.S.K.T. Adjemian, J. Benziger, A.B. Bocarsly, J. Power Sources 109 (2002) 356.
[4] M. Watanabe, H. Uchida, Y. Seki, M. Emori, J. Electrochem. Soc. 143 (1996) 3847.
[5] C. Yang, et al., Electrochem. Solid State Lett. 4 (2001) A31.
[6] P. Costamagna, C. Yang, A.B. Bocarsly, S. Srinivasan, Electrochim. Acta 27 (2002) 1023.
[7] S.M.J. Zaidi, S.U. Rahman, J. Electrochem. Soc. 152 (2005) A1594.
[8] S. Malhotra, R. Datta, J. Electrochem. Soc. 144 (1997) L23.
[9] B.T.a.O. Savadogo, Electrochim. Acta 45 (2000) 4329.
[10] B. Tazi, O. Savadogo, J. New Mater. Electrochem. Syst. 4 (2001) 187.
[11] I. Nicotera, T. Zhang, A. Bocarsly, S. Greenbaum, J. Electrochem. Soc. 154 (2007) B466.
[12] K. Miyatake, H. Iyotani, K. Yamamoto, E. Tsuchida, Macromolecules 29 (1996) 6969.
[13] Y. Yin, et al., Polymer 44 (2003) 4509.
[14] J.-M. Bae, et al., Solid State Ionics 147 (2002) 189.
[15] T. Kobayashi, M. Rikukawa, K. Sanui, N. Ogata, Solid State Ionics 106 (1998) 219.
[16] G. Alberti, M. Casciola, L. Massinelli, B. Bauer, J. Membr. Sci. 185 (2001) 73.
[17] Department of Energy, http://www1.eere.energy.gov/hydrogenandfuelcells/pdfs/htwg_rd_plan.pdf.
[18] K.D. Kreuer, Chem. Mater. 8 (1996) 610.
[19] K.D. Kreuer, S.J. Paddison, E. Spohr, M. Schuster, Chem. Rev. 104 (2004) 4637.
[20] R. Savinell, et al., J. Electrochem. Soc. 141 (1994) L46.
[21] M.F.H. Schuster, M.H. Meyer, Annu. Rev. Mater. Res. 33 (2003) 233.
[22] J.S. Wainright, J. Wang, D. Weng, R.F. Savinell, M. Litt, J. Electrochem. Soc. 142 (1995) L121.
[23] S.R. Samms, S. Wasmu, R.F. Savinell, J. Electrochem. Soc. 143 (1996) 1225.
[24] J.-T. Wang, R.F. Savinell, J. Wainright, M. Litt, H. Yu, Electrochim. Acta 41 (1996) 193.
[25] J.T. Wang, J. Wainright, R.F. Savinell, M. Litt, J. Appl. Electrochem. 26 (1996) 751.
[26] D. Weng, J.S. Wainright, U. Landau, R.F. Savinell, J. Electrochem. Soc. 143 (1996) 1260.
[27] J.J. Fontanella, M.C. Wintersgill, J.S. Wainright, R.F. Savinell, M. Litt, Electrochim. Acta. 43 (1998) 1289.
[28] R. Bouchet, E. Siebert, Solid State Ionics 118 (1999) 287.
[29] X. Glipa, B. Bonnet, B. Mula, D.J. Jones, J. Roziere, J. Mater. Chem. 9 (1999) 3045.
[30] B. Xing, O. Savadogo, J. New Mater. Electrochem. Syst. 2 (1999) 95.
[31] Q. Li, H.A. Hjuler, N.J. Bjerrum, J. Appl. Electrochem. 31 (2001) 773.
[32] M. Kawahara, J. Morita, M. Rikukawa, K. Sanui, N. Ogata, Electrochim. Acta 45 (2002) 1395.
[33] K.D. Kreuer, A. Fuchs, M. Ise, M. Spaeth, J. Maier, Electrochim. Acta 43 (1998) 1281.
[34] M. Yamada, I. Honma, Electrochim. Acta 48 (2003) 2411.
[35] G. Scharfenberger, et al., Fuel Cells 6 (2006) 237.

[36] P. Bonhote, A.P. Dias, N. Papageorgiou, K. Kalyanasundaram, M. Gratzel, Inorg. Chem. 35 (1996) 1168.
[37] J. Fuller, A.C. Breda, R.T. Carlin, J. Electroanal. Chem. 459 (1998) 29.
[38] D.R. MacFarlane, P. Meakin, J. Sun, N. Amini, M. Forsyth, J. Phys. Chem. B 103 (1999) 4164.
[39] R.D. Rogers, K.R. Seddon, Ionic Liquids: Industrial Applications for Green Chemistry, ACS Symposium Series 818, American Chemical Society, Washington, DC, 2002, 1 pp.
[40] M.A.B.H. Susan, A. Noda, S. Mitsushima, M. Watanabe, Chem. Commun. (2003) 938.
[41] M. Doyle, S.K. Choi, G. Proulx, J. Electrochem. Soc. 147 (2000) 34.
[42] R.F.d. Souza, J.C. Padilha, R.S. Gonçalves, J. Dupont, Electrochem. Comm. 5 (2003) 728.
[43] K.-J. Kim, et al., Macromol. Rapid Commun. 25 (2004) 1410.
[44] E.L. Hahn, Phys. Rev. 80 (1950) 580.
[45] E.O. Stejskal, J.E. Tanner, J. Chem. Phys. 42 (1965) 288.
[46] E.O. Stejskal, J. Chem. Phys. 43 (1965) 3597.
[47] A. Abragam, Principles of Nuclear Magnetism, Oxford University Press, 1961.
[48] H. Vogel, Phys. Z. 22 (1921) 645.
[49] G. Tamman, W. Hesse, Z. Aborg. Allg. Chem. 156 (1926) 245.
[50] G.S. Fulcher, J. Am. Ceram. Soc. 8 (1925) 339.
[51] P. Musto, F.E. Karasz, W.J. Macknight, Polymer 34 (1993) 2934.
[52] E.R. Talaty, S. Raja, V.J. Storhaug, A. Do1lle, W.R. Carper, J. Phys. Chem. B 108 (2004) 13177.
[53] S.A. Katsyuba, P.J. Dyson, E.E. Vandyukova, A.V. Chernova, A. Vidis, Helvetica Chimica Acta 87 (2004) 2556.
[54] A. Chtioui, A. Jouini, J. Chem. Crystallogr. 34 (2004) 43.
[55] S.H. Chuang, S. Bajue, S.G. Greenbaum, J. Chem. Phys. 112 (2000) 8515.
[56] J.R.P. Jayakody, et al., J. Electrochem. Soc. 154 (2007) B242.
[57] C.E. Hughes, et al., J. Phys. Chem. B 108 (2004) 13626.
[58] T. Dippel, K.D. Kreuer, J.C. Lassegues, D. Rodriguez, Solid State Ionics 61 (1993) 41.
[59] Y.-L. Ma, J.S. Wainright, M.H. Litt, R.F. Savinell, J. Electrochem. Soc. 151 (2004) A8.